Prediction of Electronic Excited States of Adsorbates on Metal Surfaces from First Principles

Thorsten Klüner,[1,2] Niranjan Govind,[1,3] Yan Alexander Wang,[1] and Emily A. Carter[1]

[1]*Department of Chemistry and Biochemistry, Box 951569, University of California, Los Angeles, California 90095-1159*

[2]*Fritz-Haber-Institut der Max-Planck-Gesellschaft, Faradayweg 4-6, 14195 Berlin, Germany*

[3]*Accelrys, 9685 Scranton Road, San Diego, California 92121-3752*

(Received 2 January 2001)

We present the first *ab initio* prediction of localized electronic excited states in a periodically infinite condensed phase, a heretofore intractable goal. In particular, we examined local excitations within a CO molecule adsorbed on Pd(111). The calculation allows a configuration interaction treatment of a local region, while its interaction with the extended condensed phase is described via an embedding potential obtained from periodic density functional theory. Our work lays the foundation of a microscopic understanding of photochemistry and spectroscopy on metal surfaces.

DOI: 10.1103/PhysRevLett.86.5954 PACS numbers: 71.15.–m, 73.20.Hb

A state-of-the-art investigation of adsorbates on well-characterized surfaces provides insight into various phenomena extending from heterogeneous catalysis to photochemistry on surfaces. The characterization of adsorption sites and energies, as well as reaction transition states and pathways, has been an active area of experimental and theoretical research in the past few years. Reference [1] contains representative papers with a focus on the system CO/Pd(111) studied in this Letter. Whereas these studies mainly focus on electronic ground state properties, the investigation of electronically excited states of adsorbates on surfaces is necessary for the understanding of surface photochemistry. Only recently has the basic mechanism of the most simple photochemical reaction (laser-induced desorption) been clarified in a combined experimental and theoretical effort for adsorbates on insulator surfaces [2]. However, the reliable calculation of excited states of adsorbates on metal surfaces remains a challenge due to the delocalized electronic structure of the substrate. To our knowledge there has been no first principles approach to the calculation of localized excited states for extended systems.

On the other hand, the investigation of ground state properties such as adsorption energies and geometries often can be performed with reasonable accuracy within a periodic density functional (DFT) or Hartree-Fock (HF) theory [3]. However, these approaches inherently omit a systematic treatment of electron correlation, since in a DFT framework the exact exchange-correlation functional is unknown and HF calculations do not include correlation effects by definition. Furthermore, a systematic treatment of local electronic excited states by DFT is by no means straightforward, although eventually a time-dependent density functional theory formalism or the *GW* approximation [4] may prove tractable in the condensed phase.

Alternatively, embedded cluster studies allow for an efficient and accurate calculation of electron correlation effects by means of configuration interaction (CI), coupled cluster or perturbation theory [5], and are able to describe excited states of adsorbates on surfaces [2,6]. Up to now, cluster models have been limited to substrates exhibiting a localized electronic structure, e.g., insulators or semiconductors such as metal oxides or silicon. The inherent lack of periodic boundary conditions in cluster calculations results in a poor description of systems with a delocalized electronic structure such as metals.

We report in this Letter a unification of density functional theory and quantum chemistry, which combines the advantages of both approaches (periodic boundary conditions and a local treatment of electron correlation *and* excited states). In our formalism, a representative region (i.e., the adsorption site), denoted as region I, contains the adsorbate and nearest neighbor surface atoms. This "cluster" region is treated by accurate quantum chemical methods, (e.g., HF, MP-n, or CI), where the influence of the environment (region II) is accounted for via a density-based embedding operator constructed from a periodic DFT calculation. A total density ρ_{tot} of the adsorbate/substrate system is obtained using a pseudopotential/plane-wave-based code [7]. This density is kept fixed in the subsequent embedded cluster study in which a HF calculation for the cluster/adsorbate system is performed as a zeroth order approximation. The effect of the environment (region II) on the cluster (region I) enters the HF equations via an effective local one-electron embedding operator $\hat{v}_{\mathrm{emb}}$. In matrix notation, the HF equations result in

$$\sum_{\nu} (F_{\mu\nu} + M_{\mu\nu}) C_{\nu,i} = \varepsilon_i \sum_{\nu} S_{\mu\nu} C_{\nu,i} \,, \qquad (1)$$

where $F_{\mu\nu}$ and $S_{\mu\nu}$ denote the Fock- and overlap-matrix elements in the Gaussian atomic orbital (AO) basis. ε_i and $C_{\nu,i}$ denote the orbital energy and the molecular orbital expansion coefficients for the ith molecular orbital, respectively. $M_{\mu\nu}$ is the matrix representation of the embedding operator in the AO basis

$$M_{\mu\nu} = \langle \phi_\mu | \hat{v}_{\mathrm{emb}} | \phi_\nu \rangle \,. \qquad (2)$$

Details about the formalism can be found elsewhere [8,9]. Very briefly, the embedding potential $\hat{v}_{\mathrm{emb}}$ resulting from

 0031-9007/01/86(26)/5954(4)$15.00

the environment (region II) is constructed in a DFT formalism by taking the difference of the potentials arising from the total system (described by the density $\rho_{\text{tot}} = \rho_{\text{I}} + \rho_{\text{II}}$) and the potentials due to region I:

$$\hat{v}_{\text{emb}} = \left(\frac{\delta T_s[\rho_{\text{tot}}]}{\delta \rho_{\text{tot}}} - \frac{\delta T_s[\rho_{\text{I}}]}{\delta \rho_{\text{I}}} \right) + (V_H^{\text{tot}} - V_H^{\text{I}}) + (V_{XC}^{\text{tot}} - V_{XC}^{\text{I}}) + (V_{NE}^{\text{tot}} - V_{NE}^{\text{I}}), \quad (3)$$

where V_H, V_{XC}, V_{NE}, and $\frac{\delta T_s[\rho]}{\delta \rho}$ denote the Hartree repulsion, exchange correlation, nuclear-electron attraction, and kinetic energy potentials, respectively. The most challenging part is the kinetic energy potential, since the exact form of the kinetic energy functional is unknown, analogous to the exact V_{XC}. The sensitivity of the theory to the choice of kinetic energy functionals will be shown later. It should be noted that V_H^{I}, V_{XC}^{I}, and V_{NE}^{I} are treated self-consistently in the solution of Eq. (1), while the remaining terms are kept fixed [9,10]. The post-HF methods, MP-n and CI, can be applied straightforwardly after the HF equations have been solved [9]. In MP-n the embedding potential is constructed using a HF density, since only a transformation of the two-electron integrals into the molecular orbital basis is necessary to calculate the MP-n energy correction. In an embedded complete active space self-consistent field (CASSCF) or CI calculation also the one-electron embedding integrals defined in Eqs. (2) and (3) have to be transformed. In our implementation the embedding potential corresponds to HF embedding operators when MP-n or CI is applied. However, in a CASSCF scheme, $v_{\text{emb}}[\rho_{\text{I}}]$ is constructed by using the CASSCF density.

In this paper, we use a three-layer slab containing eight Pd atoms per layer to model a Pd(111) surface, and a CO molecule is placed at an fcc hollow site on one side of the slab corresponding to a coverage of 0.125 monolayers (Fig. 1). Convergence studies show that a three-layer slab is sufficiently thick to accurately calculate properties such as adsorption geometries and energies. This well-studied benchmark system is ideally suited to judge the reliability of our new approach. The simulation cell, which is periodically repeated in three dimensions, was large enough (5.52 Å × 9.55 Å × 16.00 Å) so that the interactions between the periodic slab images in the direction normal to the Pd(111) surface were negligible. Nonlocal norm-conserving pseudopotentials, a plane-wave cutoff of $E_{\text{cut}} = 700$ eV, and a surface Brillouin zone sampling containing nine special k points have been used in order to obtain an accurate total density, ρ_{tot}. The substrate geometry was chosen to match the experimental bulk lattice constant. Surface relaxation effects were found to be unimportant for adsorption properties of this system. However, a full geometry optimization of the adsorbed CO molecule was performed using the PW91 gradient-corrected exchange-correlation functional [11]. This results in an adsorption energy of $\Delta E_{\text{slab}}^{\text{DFT}} = -1.71$ eV and a geometry

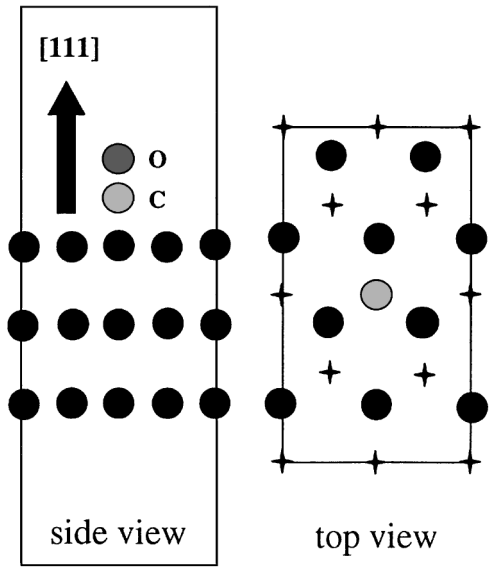

FIG. 1. Pd(111)/CO: the slab model containing three Pd layers with eight atoms per layer. The CO molecule adsorbs at an fcc hollow site with the molecular axis parallel to the surface normal. The stars indicate unoccupied fcc hollow sites.

defined by the interatomic distances d(C-O) = 1.172 Å and d(Pd-C) = 2.096 Å.

For most calculations, the cluster used in our embedding theory consists of the CO molecule and the three Pd atoms of the fcc hollow site. Cluster size convergence was investigated for excited state calculations by including three Pd atoms adjacent to the three Pd atoms of the adsorption site in the second layer, resulting in a Pd_6 cluster. In the quantum chemistry calculation, the core electrons are treated within the effective core potential approximation [12,13] and the valence electrons are described by a double zeta basis [14]. All calculations were performed using a modified version of the HONDO quantum chemical program [15].

In order to test the general validity of our approach, we first performed a DFT calculation in region I in the presence of a DFT embedding potential. According to Eq. (4) below, this simply should reproduce the DFT slab result, since the correction term in parentheses will be zero. Indeed, the resulting ground state electron density in region I is almost indistinguishable from the total density ρ_{tot} obtained from the periodic slab calculation in the same region [9]. This proves that our embedding scheme properly mimics the periodic boundary conditions necessary for a description of metallic states and justifies the use of the conventional gradient expansion for the kinetic energy potential, as well as approximation [10].

In order to test the reliability of our embedded cluster model for the subsequent excited state calculations, we first calculate a ground state property that has been measured experimentally: the adsorption energy of CO on Pd(111).

We report the adsorption energy ΔE_{ads} as a correction to the DFT results in Table I according to the following expression [8]:

TABLE I. Adsorption energy (ΔE_{ads}) for CO on Pd(111).

ΔE_{ads}/eV	Pd_3/CO Embedded	Pd_3/CO Not embedded
E(HF)	−2.13	−1.75
E(MP-2)	−1.42	−4.55
E(MP-4)	−1.55	−5.03
E_{slab}(PW91)	−1.71	
E(exp)	−1.47 to −1.54 [16]	

$$\Delta E_{ads} = \Delta E_{slab}^{DFT} + (\Delta E_I^{ab\ initio} - \Delta E_I^{DFT}). \quad (4)$$

$\Delta E_I^{ab\ initio}$ denotes the *ab initio* adsorption energy of the embedded cluster/adsorbate (region I) and ΔE_I^{DFT} denotes the adsorption energy of the adsorbed molecule calculated as the DFT energy expectation value using the converged embedded cluster density.

Table I demonstrates that the local correction ($\Delta E_I^{ab\ initio} - \Delta E_I^{DFT}$) imposed by the DFT embedding of the Pd_3 cluster significantly improves the PW91 slab adsorption energies. Within the HF approximation, the adsorption energy is overestimated but the MP-n results, which account systematically for electron correlation, correct this deficiency. At the highest level of theory (MP-4), the adsorption energy, $\Delta E_{ads} = -1.55$ eV, agrees very well with the experimental low coverage value $\Delta E_{exp} \approx -1.5$ eV [16].

Results for the nonembedded Pd_3 cluster are also reported in Table I. In the absence of the embedding potential, the quasidegeneracy of the one-particle energies, characteristic of transition metal compounds, causes quasisingularities in the many-body perturbation energy expressions, resulting in the divergence of the MP-n series.

All results reported in Table I were obtained by using the locally truncated conventional gradient expansion [17] for the kinetic energy functionals in Eq. (3), i.e.,

$$T_s = T_{TF} + 1/9 T_{vW}, \quad (5)$$

where T_{TF} and T_{vW} denote the Thomas-Fermi and von Weizsäcker kinetic energy functionals, respectively. Details on the construction of the kinetic energy potential can be found elsewhere [9]. Application of a gradient expansion for the kinetic energy functional is consistent with the treatment of the exchange-correlation functional in Eq. (3), where we applied the generalized gradient approximation. As can be seen in Table II, kinetic energy functionals such as T_{TF} or T_{ZLP} [18], which do not contain gradient corrections, give inferior results, as does a local density approximation embedding scheme [9]. Thus, use of gradient corrections in both the exchange-correlation and kinetic energy functional components of the embedding potential is essential for high accuracy.

Beyond accurate calculations of ground state adsorption energies, this method affords the means to finally calculate electronic excited states on metals. To demonstrate this, vertical excitation energies for the internal CO singlet/singlet $^1(5\sigma/1\pi \rightarrow 2\pi^*)$ transition were calculated by performing CI calculations for the systems Pd_3/CO and Pd_6/CO.

TABLE II. Adsorption energy Pd_3/CO using different kinetic energy functionals for the embedding potential.

ΔE_{ads}/eV	$T_{TF} + 1/9 T_{vW}$	T_{TF}	T_{ZLP}
E(HF)	−2.13	−1.86	−1.92
E(MP-2)	−1.42	−2.13	−2.05
E(MP-4)	−1.55	−2.21	−2.13

In order to obtain the orbitals for a subsequent CI calculation, a CASSCF [19] embedding calculation is performed, in which the active space consists of the 3σ, 4σ, 5σ, 1π, and $2\pi^*$ orbitals of the adsorbed CO molecule. A balanced description of both electronic states is achieved by constructing state-averaged orbitals for the electronic ground state and the $^1(5\sigma/1\pi \rightarrow 2\pi^*)$ excited state. The embedding operators are constructed using these state-averaged density matrices. This procedure provides embedding operators which are consistent with the state-averaged CASSCF energy functional. In a second step, the CASSCF state-averaged orbitals are used in an embedding CI calculation within the same configuration space as in the preceding CASSCF calculation, where now the embedding operators are constructed from a density matrix corresponding to the ground state closed-shell reference configuration [9]. Thus, we assume the embedding operators based on the ground state density to be applicable in excited state calculations. This procedure clearly has to be regarded as a first approximation; future studies will provide insight into its general applicability.

For Pd_3/CO and Pd_6/CO, we obtain a vertical excitation energy of 9.6 and 9.8 eV, respectively (Table III). Obviously, the results are converged with respect to the cluster size. The data can be directly compared to the experimental electron energy loss spectrum, where a feature in the experimental spectrum at 14 eV has been assigned to the $^1(5\sigma/1\pi \rightarrow 2\pi^*)$ transition [20]. Although this value is close to the calculated $^1(5\sigma/1\pi \rightarrow 2\pi^*)$ excitation energy of CO bound to Pt_2 (11.3–12.7 eV) [21], our results clearly suggest the assignment of Netzer *et al.* [20] to be incorrect. Indeed, it has been pointed out in Ref. [22] that for other substrates such as Ni(100) and Cu(110) this excitation energy is about 9 eV, which is in reasonable agreement with our result for CO/Pd(111). The slight overestimation of the vertical excitation energy is mainly due to basis set and active space limitations [9]. To underscore the importance of a proper embedding potential, nonembedded cluster calculations were performed yielding excitation energies of 3.1–4.5 eV, which are certainly too small. This is due to the insufficient description of the Pauli repulsion between the metal surface and the $2\pi^*$ orbital of CO when no embedding potential is applied. The presence of the extended surface raises the energy of the $2\pi^*$ orbital, resulting in a significantly higher excitation energy when our embedding scheme is used.

In conclusion, we report a new density-based embedded cluster approach that efficiently bridges the gap between periodic DFT and quantum chemical cluster calculations.

TABLE III. Vertical excitation energy for the $^1(5\sigma/1\pi \rightarrow 2\pi^*)$ transition: CASSCF(10/7)/CI.

ΔE/eV	Pd_3/CO	Pd_6/CO
With embedding	9.6	9.8
Without embedding	4.5	(3.1) [23]

For the benchmark system CO/Pd(111), we were able to accurately reproduce not only the adsorption energy of the CO molecule but further to predict the energy of a localized electronic transition corresponding to a $^1(5\sigma/1\pi \rightarrow 2\pi^*)$ excitation within the adsorbed molecule. This opens the way more generally for the calculation of local excited states in bulk metals and on metal surfaces.

Financial support from the U.S. National Science Foundation (NSF), the Air Force Office of Scientific Research, the Army Research Office, and the Deutsche Forschungsgemeinschaft (DFG) is gratefully acknowledged.

[1] P. Sautet, M. K. Rose, J. C. Dunphy, S. Behler, and M. Salmeron, Surf. Sci. **453**, 25 (2000); D. Loffreda, D. Simon, and P. Sautet, Surf. Sci. **425**, 68 (1999); P. H. T. Philipsen, E. van Lenthe, J. G. Snijders, and E. J. Baerends, Phys. Rev. B **56**, 13 556 (1997); A. M. Bradshaw and F. M. Hoffmann, Surf. Sci. **72**, 513 (1978); M. Tüshaus, W. Berndt, H. Conrad, A. M. Bradshaw, and B. Persson, Appl. Phys. A **51**, 91 (1990); P. S. Bagus, C. J. Nelin, and C. W. Bauschlicher, Jr., Phys. Rev. B **28**, 5423 (1983); G. Pacchioni and J. Koutecký, J. Phys. Chem. **91**, 2658 (1987); B. Hammer, L. B. Hansen, and J. K. Nørskov, Phys. Rev. B **59**, 7413 (1999).

[2] T. Mull, B. Baumeister, M. Menges, H.-J. Freund, D. Weide, C. Fischer, and P. Andresen, J. Chem. Phys. **96**, 7108 (1992); T. Klüner, H.-J. Freund, V. Staemmler, and R. Kosloff, Phys. Rev. Lett. **80**, 5208 (1998); T. Klüner, S. Thiel, H.-J. Freund, and V. Staemmler, Chem. Phys. Lett. **294**, 413 (1998).

[3] C. Pisani, R. Dovesi, C. Roetti, M. Causà, R. Orlando, S. Casassa, and V. R. Saunders, Int. J. Quantum Chem. **77**, 1032 (2000); A. Eichler, J. Hafner, A. Groß, and M. Scheffler, Phys. Rev. B **59**, 13 297 (1999); A. Bogicevic, S. Ovesson, P. Hyldgaard, B. I. Lundqvist, H. Brune, and D. R. Jennison, Phys. Rev. Lett. **85**, 1910 (2000).

[4] E. K. U. Gross and W. Kohn, Adv. Quantum Chem. **21**, 255 (1990); H. H. Heinze, A. Görling, and N. Rösch, J. Chem. Phys. **113**, 2088 (2000); M. E. Casida, F. Gutierrez, J. Guan, F.-X. Gadea, D. Salahub, and J.-P. Daudey, J. Chem. Phys. **113**, 7062 (2000); N. C. Handy and D. J. Tozer, J. Comput. Chem. **20**, 106 (1999); L. Hedin, Phys. Rev. **139**, A796 (1965); M. S. Hybertsen and S. G. Louie, Phys. Rev. Lett. **55**, 1418 (1985); R. W. Godby and L. J. Sham, Phys. Rev. B **49**, 1849 (1994).

[5] Y. Fukunishi and H. Nakatsuji, J. Chem. Phys. **97**, 6535 (1992); H. A. Duarte and D. R. Salahub, J. Chem. Phys. **108**, 743 (1998); J. L. Whitten and T. A. Pakkanen, Phys. Rev. B **21**, 4357 (1980); I. V. Abarenkov, V. L. Bulatov, R. Godby, V. Heine, M. C. Payne, P. V. Souchko, A. V. Titov, and I. I. Tupitsyn, Phys. Rev. B **56**, 1743 (1997); P. Cortona, Phys. Rev. B **44**, 8454 (1991); J. R. Trail and D. M. Bird, Phys. Rev. B **62**, 16 402 (2000); D. E. Ellis, G. A. Benesh, and E. Byrom, J. Appl. Phys. **49**, 1543 (1978); T. N. Truong and E. V. Stefanovich, Chem. Phys. Lett. **240**, 253 (1995).

[6] A. Freitag, V. Staemmler, D. Cappus, C. A. Ventrice, Jr., K. Al-Shamery, H. Kuhlenbeck, and H.-J. Freund, Chem. Phys. Lett. **210**, 10 (1993).

[7] M. C. Payne, M. P. Teter, D. C. Allan, T. A. Arias, and J. D. Joannopoulos, Rev. Mod. Phys. **64**, 1045 (1992); Molecular Simulations, Inc., San Diego, California, CASTEP program.

[8] N. Govind, Y. A. Wang, and E. A. Carter, J. Chem. Phys. **110**, 7677 (1999); N. Govind, Y. A. Wang, A. J. R. da Silva, and E. A. Carter, Chem. Phys. Lett. **295**, 129 (1998).

[9] T. Klüner, N. Govind, Y. A. Wang, and E. A. Carter (to be published).

[10] $\frac{\delta T_s[\rho_1]}{\delta \rho_1}$, the kinetic energy potential, is obtained from a nonembedded cluster calculation and kept fixed in the iterative solution of the embedded HF equations. The insertion of "good" densities in the conventional gradient expansion results in more accurate kinetic energies compared to self-consistent solutions; we believe this is true also for the kinetic energy potential. For a detailed discussion, see R. M. Dreizler and E. K. U. Gross, *Density Functional Theory* (Springer-Verlag, Berlin, 1990), p. 98.

[11] J. P. Perdew, J. A. Chevary, S. H. Vosko, K. A. Jackson, M. R. Pederson, D. J. Singh, and C. Fiolhais, Phys. Rev. B **46**, 6671 (1992).

[12] P. J. Hay and W. R. Wadt, J. Chem. Phys. **82**, 270 (1985).

[13] W. J. Stevens, H. Basch, and M. Krauss, J. Chem. Phys. **81**, 6026 (1984).

[14] Pd: $3s3p4d/2s2p2d$ from Ref. [12]. C,O: $4s4p/2s2p$ from Ref. [13] augmented by $1d(0.8) + 1p(0.05)$.

[15] M. Dupuis, A. Marquez, and E. R. Davidson, "HONDO 95.3 from CHEM-Station," IBM Corporation, Neighborhood Road, Kingston, New York (1995).

[16] H. Conrad, G. Ertl, J. Koch, and E. E. Latta, Surf. Sci. **43**, 462 (1974); X. Guo and J. T. Yates, Jr., J. Chem. Phys. **90**, 6761 (1989).

[17] P. Hohenberg and W. Kohn, Phys. Rev. **136**, B864 (1964).

[18] Q. Zhao, M. Levy, and R. G. Parr, Phys. Rev. A **47**, 918 (1993).

[19] A CASSCF calculation consists of a simultaneous optimization of molecular orbital expansion coefficients and CI coefficients for a full CI in the active space.

[20] F. P. Netzer and M. M. El Gomati, Surf. Sci. **124**, 26 (1983); S. D. Bader, J. M. Blakely, M. B. Brodsky, R. J. Friddle, and R. L. Panosh, Surf. Sci. **74**, 405 (1978).

[21] H. Nakatsuji, H. Morita, H. Nakai, Y. Murata, and K. Fukutani, J. Chem. Phys. **104**, 714 (1996).

[22] P. Avouris and J. E. Demuth, Surf. Sci. **158**, 21 (1985); H.-J. Freund, R. P. Messmer, W. Spiess, H. Behner, G. Wedler, and C. M. Kao, Phys. Rev. B **33**, 5228 (1986).

[23] Because of large mixing of the CO and Pd orbitals in a state-averaged scheme, the excitation energy of the nonembedded Pd_6/CO cluster was obtained by optimizing the orbitals of each state separately. Therefore it cannot be compared directly with the state-averaged results reported in Table III.